Original Article

Long-term high fat diet aggravates the risk of lung fibrosis and lung cancer: transcriptomic analysis in the lung tissues of obese mice

Jihyun Park[1#^], Danbi Jo[2#^], Seo Yoon Choi[2,3^], Sumin Oh[1^], Yoon Seok Jung[2^], Oh Yoen Kim[1,4*^], Juhyun Song[2,3*^]

[1]Department of Health Sciences, Graduate School of Dong-A University, Busan, Republic of Korea; [2]Department of Anatomy, Chonnam National University Medical School, Hwasun, Republic of Korea; [3]Biomedical Science Graduate Program (BMSGP), Chonnam National University, Hwasun, Republic of Korea; [4]Department of Food Science and Nutrition, College of Health Science, Dong-A University, Busan, Republic of Korea

Contributions: (I) Conception and design: OY Kim, J Song; (II) Administrative support: OY Kim, J Song; (III) Provision of study materials or patients: All authors; (IV) Collection and assembly of data: All authors; (V) Data analysis and interpretation: J Park, D Jo, OY Kim, J Song; (VI) Manuscript writing: All authors; (VII) Final approval of manuscript: All authors.

[#]These authors contributed equally to this work as co-first authors.

[*]These authors contributed equally to this work.

Correspondence to: Oh Yoen Kim, PhD. Department of Food Science and Nutrition, College of Health Science, Dong-A University, Sahagu, Nakdongdaero 550 beon-gil, 49315, Busan, Republic of Korea; Department of Health Sciences, Graduate School of Dong-A University, Sahagu, Nakdongdaero 550 beon-gil, 49315, Busan, Republic of Korea. Email: oykim@dau.ac.kr; Juhyun Song, PhD. Department of Anatomy, Chonnam National University Medical School, Seoyangro 264, Hwasun 58128, Jeollanam-do, Republic of Korea; Biomedical Science Graduate Program (BMSGP), Chonnam National University, Seoyangro 264, Hwasun 58128, Republic of Korea. Email: juhyunsong@chonnam.ac.kr.

Background: Previous studies reported significant relationships between obesity and pulmonary dysfunction. Here, we investigated genetic alterations in the lung tissues of high fat diet (HFD) induced obese mouse through transcriptomic and molecular analyses.

Methods: Eight-week-old male C57BL/6J mice were fed either a normal chow diet (NCD) or HFD for 12 weeks. We performed RNA sequencing, functional analysis of altered genes using Gene Ontology (GO) and Kyoto Encyclopedia of Genes and Genomes (KEGG) pathway data, Database for Annotation, Visualization and Integrated Discovery (DAVID) analysis, protein network analysis, quantitative real-time polymerase chain reaction, and Western blotting.

Results: We performed RNA sequencing analysis in the lung tissue of HFD mice. GO and KEGG pathway data presented higher expressions of genes related to lung fibrosis, and the changes of several pathways including regulation of nitrogen compound metabolic process, G protein-coupled receptor signaling, cancer pathway, and small cell lung cancer pathway. DAVID analysis and protein network analysis showed the changes of vascular endothelial growth factor, hypoxia-inducible factor-1 and rat sarcoma virus signaling related to vascular permeability, and protein network of MYC proto-oncogene gene related to cancer. In addition, we found increased protein and mRNA levels of the growth/differentiation factor 15 and alpha smooth muscle actin genes related to lung fibrosis in lung tissue of HFD mice.

Conclusions: HFD contributes to an increased risk of lung fibrosis and lung cancer. Thus, we propose that the genetic modulation and the molecular regulation of target pathways are essential to suppress pulmonary fibrosis in obese patients.

Keywords: High fat diet (HFD); obesity; lung fibrosis; lung cancer; transcriptomic analysis

^ ORCID: Jihyun Park, 0000-0003-1038-2586; Danbi Jo, 0000-0003-0013-9291; Seo Yoon Choi, 0009-0009-9179-5542; Sumin Oh, 0009-0007-9401-9448; Yoon Seok Jung, 0000-0002-4539-925X; Oh Yoen Kim, 0000-0001-9262-3309; Juhyun Song, 0000-0002-9165-8507.

Submitted Jul 30, 2024. Accepted for publication Nov 26, 2024. Published online Dec 27, 2024.
doi: 10.21037/tlcr-24-659
View this article at: https://dx.doi.org/10.21037/tlcr-24-659

Introduction

The prevalence of obesity and overweight is dramatically increasing worldwide, with a greater acceleration than ever before (1). Obesity is linked to the development of metabolic diseases, such as type 2 diabetes and cardiovascular disease, and the increased risk of various cancers, including lung cancer (2). Recent study has focused on the relationship between central obesity and lung cancer progression and many have attempted to understand their relationship (3). However, the relationship between obesity and lung cancer has remained controversial until now. Some cohort study has reported that a high body mass index (BMI) may reduce the risk of lung cancer (4), while a low BMI increases the risk of lung cancer (5). In contrast, other studies have demonstrated that the body fat distribution is a more sensitive contributor to respiratory function than BMI alone (3,6). Lung fibrosis, which leads to lung structure remodeling and functional respiratory impairment, is observed approximately twice as often in obese people than in healthy people (7). Indeed, a previous study reported that high fat intake, particularly a high consumption of saturated fatty acids, increases the risk of idiopathic pulmonary fibrosis, a type of interstitial lung disorder (8).

In overweight and obese individuals, the mechanical features of the lungs and chest wall are considerably changed owing to excessive fat deposits in the mediastinum and abdominal cavities, which subsequently lead to impaired respiratory symptoms such as wheeze and dyspnea (9). Obesity also reduces functional residual capacity, expiratory reserve volume, and total lung capacity (10). Obese animals also exhibit a reduced nasopharyngeal volume, smaller airways (11), and pulmonary inflammation (12). As mentioned above, numerous studies have provided extensive evidence for the relationship between obesity and lung function; however, the specific genetic alterations in the lung tissues of obese status induced by a high fat diet (HFD) are poorly understood. Therefore, in this study, we investigated the transcriptomic analysis and molecular analysis in the lung tissues of HFD induced obese mouse model. We present this article in accordance with the ARRIVE reporting checklist (available at https://tlcr.amegroups.com/article/view/10.21037/tlcr-24-659/rc).

Highlight box

Key findings

- Our results showed the genetic alteration and the changes of significant molecular signaling of the lung tissue in the high fat diet (HFD) fed mice.
- HFD-induced obesity contributes to an increased risk of lung fibrosis and lung cancer.

What is known and what is new?

- Obesity is related to the development of metabolic diseases such as type 2 diabetes and cardiovascular disease, as well as increased risk of cancers including lung cancer.
- Furthermore, high fat intake may increase the risk of several lung diseases.
- We found significantly distinct alteration of the genes and proteins related to lung fibrosis and lung cancer expressed in the lung tissues of HFD-induced obese mice compared to those in control tissues.

What is the implication, and what should change now?

- These results propose that the genetic modulation and the molecular regulation of target pathways are essential to suppress pulmonary fibrosis in obese patients.
- Further studies are needed to elucidate the effect of HFD-induced obesity on the risk of lung fibrosis and lung cancer in humans including healthy people and patients with lung disease.

Methods

Preparation of samples from HFD induced obese mice model

Eight-week-old male C57BL/6J mice maintained by Jackson Laboratories (Orient Science, Bar Harbor, ME, USA) were used for the experiments. The mice were fed either normal chow diet (NCD) 6 mice or HFD 6 mice (Rodent Diet with 45 kcal % fat, research diets) for 12 weeks (Figure S1A). Body weight and glucose levels in blood were checked every week for the 12-week NCD or HFD treatment. Mouse glucose level was measured once a week. Blood samples were collected from the tip of tail, and the immediately glucose level was measured using a glucocare (G400 glucocare blood glucose monitoring system, GCbiopharma, Yongin, Republic of Korea) (13). To take out lung tissues, the mice were sacrificed under their anesthesia using

2,2,2-tribromoethanol/2-methyl-2-butanol (Sigma Aldrich, St. Louis, MO, USA) 0.2 mg/g (body weight) through an intraperitoneal injection. Experiments were performed under a project license (CNU IACUC-H-2022-8) granted by Animal Ethics Committee of Chonnam National University (CNU), in compliance with the 96 Guidance for Animal Experiments for the care and use of animals.

RNA sequencing analysis

Total RNA was extracted from the lung tissue of HFD fed mice using TRIzol reagent (Thermo Fisher, Waltham, MA, USA) and RNA's integrity was measured using an Agilent 2100 BioAnalyzer (Agilent, Santa Clara, CA, USA). Total RNA was applied to a Ribo-Zero Gold rRNA Removal Kit (Illumina, San Diego, CA, USA) to eliminate ribosomal RNA. The RNA sequencing libraries were ready using a TruSeq Stranded Total RNA Kit (Illumina). The RNA libraries were paired-end sequenced with 100 sequencing cycles on a HiSeq 2500 system (Illumina).

General analysis of RNA sequencing data

Low-quality reads from the RNA sequencing data were deleted using Trimmomatic (11). The trimmed sequences were aligned to the mouse genome (mm10) through the spliced transcripts alignment to a reference (STAR) aligner (14). Cuffnorm was used to test the normalized fragments per kilobase of transcript per million mapped reads (FPKM) values regarding the GENCODE annotation (Release M17, GRCm38.p6) (15). Transcripts with mean FPKM values <1 and those that were not assessed in any samples were left out from further analysis.

Functional analysis of altered genes

Differential gene expression analysis was performed using Student's *t*-test to identify genes showing significant expression changes between HFD and control groups ($P<0.05$). This analysis identified 1,506 genes with significant expression alterations. From these statistically significant genes, we selected the top ten increased and decreased genes based on their fold changes. We conducted Gene Ontology (GO) analysis using the Molecular Signatures Database (16) by sequentially applying 500 genes selected from lung tissues in the order of statistical significance. Among the significantly altered genes, gene-gene interaction network analysis was performed using STRING (http://string-db.org) for the top 200 significant genes, and the GeneMANIA plugin in Cytoscape was used for visualization (17,18). Functional annotation clustering was conducted using the Database for Annotation, Visualization and Integrated Discovery (DAVID) tool (19) for the top 500 significant genes.

Quantitative real-time polymerase chain reaction (RT-PCR)

Total RNA was gained using TRIzol reagent (Ambion, Austin, TX, USA) following the manufacturer's instructions, and complementary DNA (cDNA) was reverse-transcribed from the extracted RNA using RevertAid reverse transcriptase (Thermo Fisher Scientific, Waltham, MA, USA). The cDNA quantification was carried out using a NanoPhotometer (IMPLEN, Westlake village, CA, USA). Quantitative RT-PCR was carried out using 10 ng of cDNA with the SYBR green PCR master mix and the Step One Plus real-time PCR system (Applied Biosystems, Foster City, CA, USA). Each gene expression level was normalized relative to the expression level of glyceraldehyde 3-phosphate dehydrogenase (Gapdh). The mRNA levels of transforming growth factor β (Tgfβ), α-smooth muscle actin (αSMA), collagen type I alpha 1 chain (Col1a1), platelet-derived growth factor receptors (Pdgfr), Tissue inhibitor matrix metalloproteinase 1 (Timp1), growth differentiation factor 15 (Gdf15), and glial cell-derived neurotrophic factor family receptor alpha-like (Gfral) genes were normalized to the *Gapdh* expression levels. The following PCR primers were used: Tgfβ (mouse), 5'-CTCCCGTGGCTTCTAGTGC-3' (forward) and 5'-GCCTTAGTTTGGACAGGATCTG-3' (reverse); αSma (mouse), 5'-AACGCCTTCCGCTGCCC-3' (forward) and 5'-CGATGCCCGCTGACTCC-3' (reverse); Col1a1 (mouse), 5'-GCTCCTCTTAGGGGCCACT-3' (forward) and 5'-CCACGTCTCACCATTGGGG-3' (reverse); Pdgfr (mouse), 5'-TTCCAGGAGTGATACCAGCTT-3' (forward) and 5'-AGGGGGCGTGATGACTAGG-3' (reverse); Timp1 (mouse), 5'-GCAACTCGGACCTGGTCATAA-3' (forward) and 5'-CGGCCCGTGATGAGAAACT-3' (reverse); Gdf15 (mouse), 5'-AGCCGAGAGGACTCGAACTCAG-3' (forward) and 5'-GGTTGACGCGGAGTAGCAGCT-3' (reverse); Gfral (mouse), 5'-TTCCTGGCTGTTACGTTAAGC-3' (forward) and 5'-GCCATTTGCATCAATCAAGCA-3' (reverse); Gapdh (mouse), 5'-AATGTGTCCGTCGTGGATCT-3' (forward) and 5'-AGACAACCTGGTCCTCAGTG-3' (reverse) (Table S1).

Western blot analysis

The lung tissues of mice were lysed with RIPA buffer (Translab, Bangalore, KA, India) with 1× phosphatase inhibitor and 1× protease inhibitor for 20 min. The protein concentrations were quantified using a BCA assay kit (Thermo Fisher Scientific) following the manufacturer's instructions. Proteins (25 µg) were electrophoresed on 8–10% sodium dodecyl sulfate-polyacrylamide gel (SDS-PAGE), before transferring onto a methanol-activated polyvinylidene difluoride (PVDF) membrane. The membrane was blocked with 5% bovine serum albumin (GenDEPOT, Altair, TX, USA) or 5% skim milk (BDsciences, Franklin Lakes, NJ, USA) for 1 h 30 min at room temperature, continually incubation with primary antibodies (1:1,000) against phospho-AKT (Ser473, Cell Signaling, Danvers, MA, USA), AKT (Cell Signaling), β-catenin (Cell Signaling), GDF15 (Abcam), αSMA (Cell Signaling), matrix metalloproteinase-9 (MMP-9) (Cell Signaling), PDK4 (Novus biologicals, Littleton, CO, USA), leucine zipper tumor suppressor 1 (LZTS1) (Novus biologicals), cytochrome p450 cytochrome p450 26b1 (Cyp26b1) (Novus biologicals) and GAPDH (Santa Cruz, CA, USA) overnight at 4 ℃. Next, the membranes were incubated with HRP-conjugated secondary antibody (1:5,000) for 2 h at room temperature. Finally, ECL solution (Thermo Fisher Scientific) was treated to the membranes, and then visualized using Fusion Solo software (Vilber, Marne-la-vallée, Ile-de-France, France). Protein expression was assessed using ImageJ software and normalized to GAPDH and native protein expression levels.

Statistical analysis

All data from the animal study are exhibited as the group mean ± standard error (SE). Statistical analysis was performed using an unpaired two-tailed *t*-test with Welch's correction in GraphPad Prism 8 (GraphPad Software Inc, USA) and Mann-Whitney test (non-parametric *t*-test) in SPSS version 27.0 (SPSS Inc., Chicago, IL, USA). Data were regarded as significant at $P<0.05$.

Results

Metabolic changes of NCD or HFD fed mice

Body weight and blood glucose levels were measured every week for the 12-week NCD or HFD treatment (Figure S1B,S1C). Body weights of the HFD fed mice (C57BL/6J) were significantly and gradually increased than those of the NCD fed mice since 6th week of the treatment. Blood glucose levels were generally higher in the HFD fed mice than the NCD fed mice. Statistical significances were observed at 2nd, 4th, and 9th–12th week of the treatment.

Transcriptome analysis in the lung tissue of NCD or HFD fed mice

The RNA sequencing analysis was performed in the lung tissues of the NCD or HFD fed mice. The RNA sequencing data were well grouped by diet type (NCD and HFD) (*Figure 1A*). The genes with higher expression levels and statistically significant alterations in each diet group were shown as volcano plots (*Figure 1B*). As depicted in the volcano plot, the expression of alpha tocopherol transfer protein (*Ttpa*), pyruvate dehydrogenase kinase 4 (*Pdk4*), angiopoietin like 4 (*Angptl4*), transformation related protein 53 inducible nuclear protein 1 (*Trp53inp1*), ribosomal protein L10, pseudogene 3 (*Rpl10-ps3*), fk506 binding protein 5 (*Fkbp5*), predicted gene 13940 (*Gm13940*), serine peptidase inhibitor clade A, member 3f (*Serpina3f*), zinc finger and BTB domain containing 16 (*Zbtb16*), *Gm42929*, pleckstrin homology domain containing A6 (*Plekha6*), transmembrane protein 151A (*Tmem151a*), *Gm37539*, *Gm43506*, *Lzts1*, thyroid hormone responsive (*Thrsp*), *Gm11719*, *Cyp26b1*, *Gm20631*, retinol binding protein 7 (*Rbp7*) were significantly changed in the lung tissues of HFD fed mice (*Figure 1B*). Analysis of the HFD fed mice revealed 626 and 880 genes with significantly increased and decreased expression, respectively ($P<0.05$).

Among the genes with a P value ≤0.05 in the lung tissues of the HFD fed mice, we selected the top 15 increased and decreased genes in order of the largest and smallest fold change, respectively (*Figure 1C,1D*). The top 15 increased genes included *Serpina3f*, *Rpl10-ps3*, *Zbtb16*, *Gm13940*, *Fkbp5*, H2A clustered histone 7 (*H2ac7*), hypoxia inducible factor 3 subunit alpha (*Hif3a*), heat shock protein family E (Hsp10) member 1, pseudogene 2 (*Hspe1-ps2*), *Pdk4*, G protein-coupled receptor class C group 6 member A (*Gprc6a*), *Angptl4*, lysyl oxidase (*Lox*), cadherin 17 (*Cd17*), phosphodiesterase 2A (*Pde2a*), and *Gm15501* (*Figure 1C*). The top 15 decreased genes included *Thrsp*, *Rbp7*, *Gm20631*, *Gm11719*, *Lzts1*, *Gm37539*, *Gm37612*, *Gm42929*, *Cyp26b1*, neurexophilin 3 (*Nxph3*), *Gm6855*, wingless-related integration site family member 7A (*Wnt7a*), glucagon like

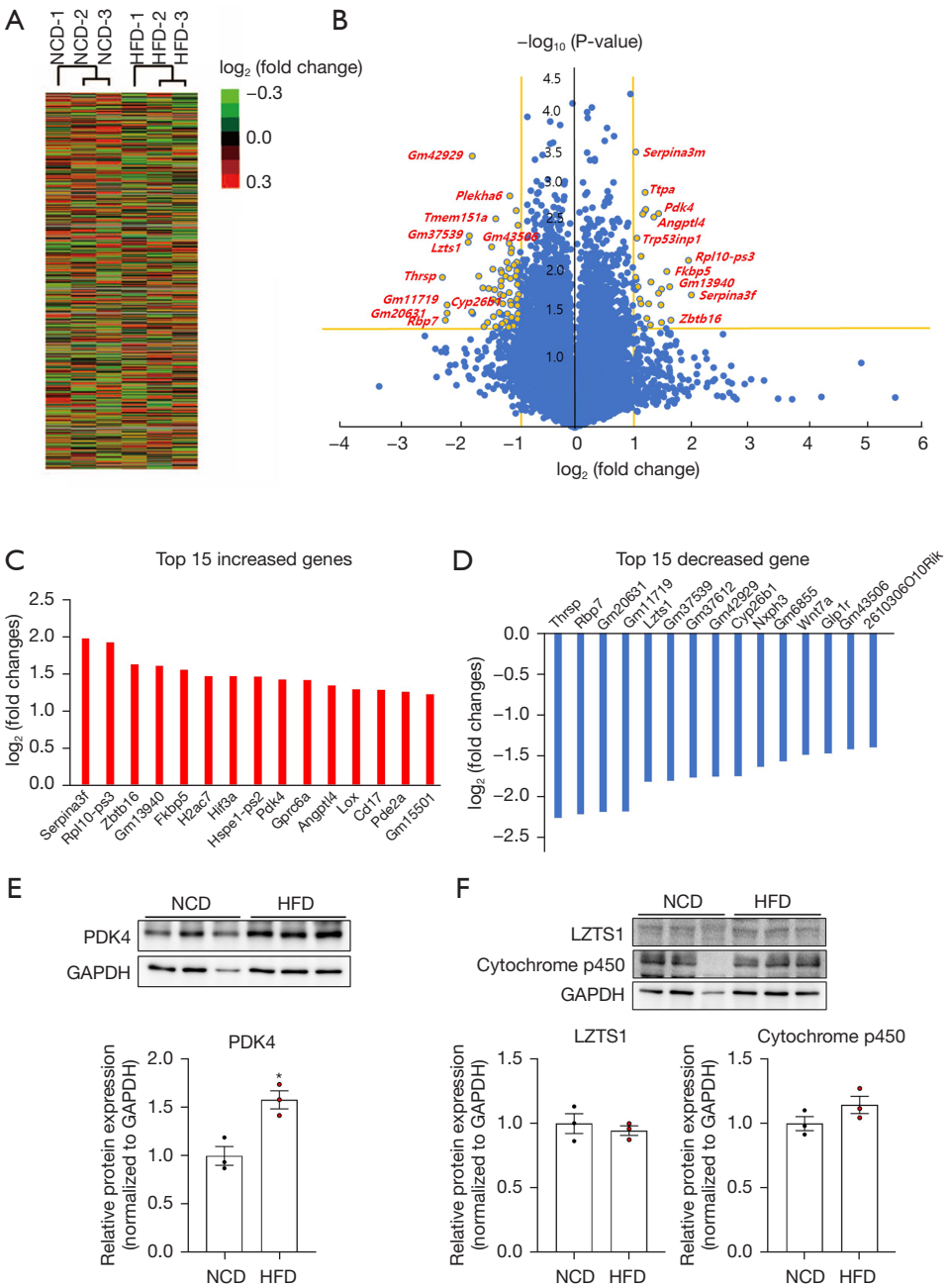

Figure 1 Analysis of the transcriptomic data from the lung tissues from HFD model mice. (A) Heatmap confirming the grouping between groups; (B) volcano plots of the HFD mouse group. The X-axis indicates the $\log_2$-transformed fold change in each group, and the Y-axis represents the $-\log_{10}$(P value) value. The vertical yellow bar indicates the $-\log_2$(fold change) of 1, while the horizontal yellow bar indicates the $-\log_{10}$(P value) of 1.3, respectively. Blue dots depict all genes expression. Yellow dots depict the significantly changed genes. (C,D) The top 15 genes with significant changes in expression in the lung tissues of HFD model mice. The graphs depict the top 15 genes with the highest fold change (C) and smallest fold change (D) among genes with P values <0.05. (E) The protein levels of PDK4, and (F) LZTS1 and cytochrome p450 Cyp26b1 in the lung tissues of NCD and HFD mice (n=3) using western blot analysis. Data are presented as the mean ± SEM (n=3). An unpaired two-tailed *t*-test with Welch's correction was used for statistical analysis. *, P<0.05. HFD, high-fat diet mice group; PDK4, pyruvate dehydrogenase kinase; LZTS1, leucine zipper tumor suppressor 1; GAPDH, glyceraldehyde 3-phosphate dehydrogenase; NCD, normal chow diet mice group; SEM, standard error of the mean.

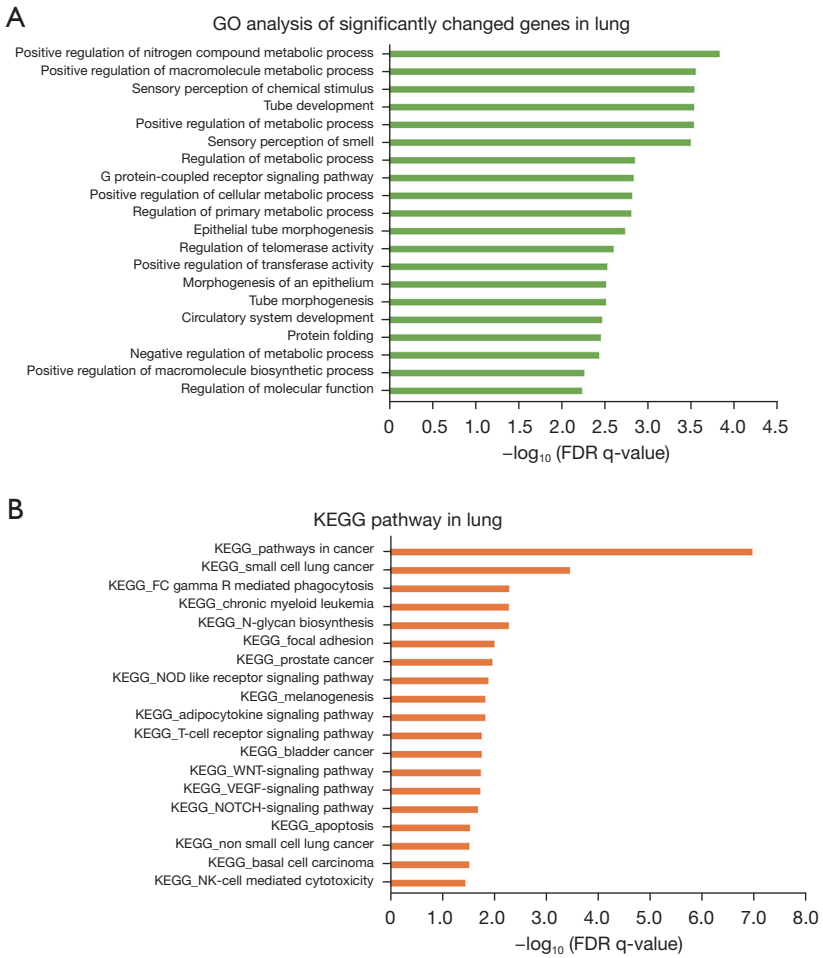

Figure 2 Functional analysis of the changed genes in the lung tissues of HFD model mice. (A) GO analysis of the changed genes in the lung tissues of HFD model mice. The top 20 GO terms based on the FDR q-value are shown. (B) KEGG pathway for the changed genes in lung tissues of HFD model mice. KEGG pathway terms based on FDR q-value are shown. GO, Gene Ontology; HFD, high-fat diet mice group; KEGG, Kyoto Encyclopedia of Genes and Genomes; FDR, false discovery rate; VEGF, vascular endothelial growth factor; NOTCH, neurogenic locus notch homolog protein; WNT, wingless-related integration site; NK, natural killer; NOD, nucleotide oligomerization domain; FC, fragment crystallizable.

peptide 1 receptor (*Glp1r*), *Gm43506*, and *2610306O10Rik* (*Figure 1D*). Among top 15 increased genes, we confirmed the protein level of PDK4 (*Figure 1E*). The protein level of PDK4 was significantly increased in the lung tissue of HFD fed mice (*Figure 1E*). Also, among top 15 decreased genes, we detected the protein levels of LZTS1 and cytochrome p450 Cyp26b1 as a representative (*Figure 1F*). The protein level of LZTS1 was slightly decreased in the lung tissue of HFD, while the protein level of cytochrome p450 Cyp26b1 was increased in the lung tissue of HFD (*Figure 1F*).

GO and KEGG analyses for the cellular pathways of associated changed genes in the lung tissue of the HFD fed mice

GO and KEGG analyses in MSigDB were performed to identify the cellular pathways associated with the genes that were altered in the lung tissues of HFD fed mice (*Figure 2A,2B*). Among the genes with a P value ≤0.05, 500 genes were selected in order of decreasing p-value. GO analysis of the significantly changed genes revealed

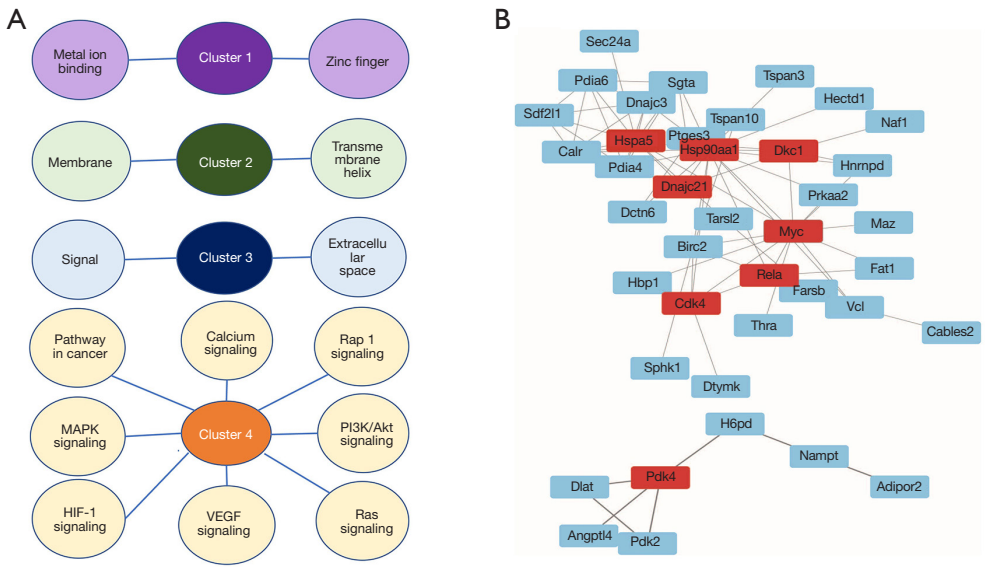

Figure 3 DAVID analysis and protein network analysis. (A) DAVID analysis of changed genes. Functional annotation clustering based on the DAVID analysis tool. The top four clusters with significant change are shown. (B) Transcriptional analysis of the changed genes in the HFD group. Signal networking data. Red boxes highlight proteins that exhibit relatively high connectivity with other proteins in the interaction network. DAVID, Database for Annotation, Visualization and Integrated Discovery; HFD, high-fat diet mice group; VEGF, vascular endothelial growth factor; MAPK, mitogen-activated protein kinase; PI3K, phosphatidylinositol 3-kinase; Akt, protein kinase B; HIF-1, hypoxia-inducible factor-1.

that there were the most significantly enriched GO terms related to positive regulation of the nitrogen compound metabolic process, macromolecular biosynthetic process, macromolecular metabolic process, and metabolic process, as well as G protein coupled receptor signaling pathway, regulation of telomerase activity, epithelial tube morphogenesis, morphogenesis of an epithelium, circulatory system development (*Figure 2A*). Additionally, KEGG analysis of the significantly changed genes in HFD fed mice revealed enrichment in cellular pathways in cancer, small cell lung cancer, fragment crystallizable (FC) gamma R mediated phagocytosis, N-glycan biosynthesis, focal adhesion, nucleotide oligomerization domain (NOD)-like receptor signaling pathway, adipocytokine signaling pathway, T-cell receptor signaling pathway, WNT signaling pathway, vascular endothelial growth factor (VEGF) signaling pathway, neurogenic locus notch homolog protein (NOTCH) signaling pathway, apoptosis, non-small cell lung cancer, and natural killer cell (NK-cell) mediated cytotoxicity (*Figure 2B*).

Functional clustering analysis of significant genes in the lung tissue of the HFD fed mice using DAVID analysis and protein network analysis

The DAVID functional annotation tool was conducted for functional clustering analysis of significant genes among 500 genes selected in order of decreasing P value among genes with a P value of ≤0.05 for the change in expression in HFD fed mice (*Figure 3A*). As a result, we observed four highly enriched clusters, one of which was related to apoptosis and cancer pathways, including phosphatidylinositol 3-kinase (PI3K)/protein kinase B (Akt) signaling, Rap1 signaling, hypoxia-inducible factor-1 (HIF-1) signaling, VEGF signaling, and Ras signaling (*Figure 3A*). Next, the STRING tool was used for the analysis of the connection among the selected 200 genes expressed in the lungs of HFD model mice in order of decreasing P value among genes with a P value of ≤0.05 for the change in expression in HFD model mice (*Figure 3B*). Among the genes, *Hspa5*, *Hsp90aa1*, *Dkc1*, *Dnajc21*, *Myc*, *Rela*, *Cdk4*, and *Pdk4* were shown to be central hubs with many connections with other genes (*Figure 3B*).

Increased expression of mRNA and protein of lung fibrosis-related genes in the lung tissues of the HFD fed mice

RT-PCR and western blotting analyses were performed to confirm the expression of lung fibrosis-related genes and their associated proteins, respectively (*Figure 4A*). Our results demonstrated significantly increased mRNA levels

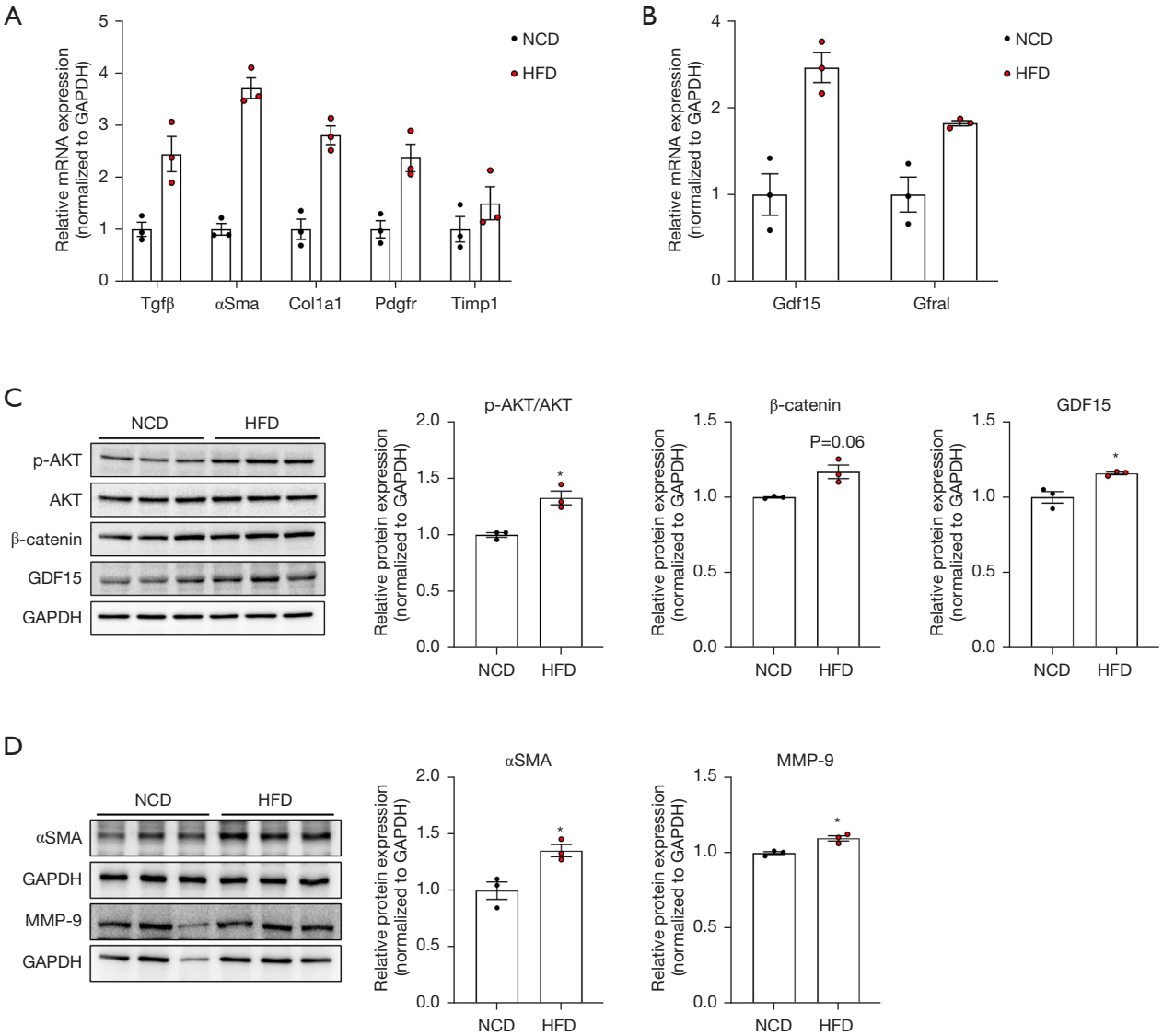

Figure 4 mRNA levels and protein levels of pulmonary fibrosis-related genes in the lungs of HFD mice. (A) The measurement of Tgfβ, αSma, Col1a1, Pdgfr and Timp1 mRNA levels in the lung tissues of HFD model mice. Data are presented as the mean ± SEM (n=3). An unpaired two-tailed *t*-test with Welch's correction was used for statistical analysis. (B) The measurement of Gdf15, and Gfral mRNA levels in the lung tissues of HFD model mice. Data are presented as mean ± SEM (n=3). An unpaired two-tailed *t*-test with Welch's correction was used for statistical analysis. (C) Western blot analysis of AKT signaling pathway and pulmonary fibrosis markers (β-catenin, and GDF15) in the lung tissues of NCD and HFD mice (n=6). (D) Western blot analysis of lung fibrosis markers (αSMA and MMP-9) in the lung tissues of NCD and HFD mice (n=6). Protein expression was normalized to GAPDH and native protein levels. Data are expressed as mean ± SEM. Statistical analysis was conducted to determine the relative significance between the NCD and the HFD groups (unpaired two-tail *t*-test with Welch's correction); *, P<0.05. TGFβ, transforming growth factor β; αSMA, α-smooth muscle actin; Col1a1, collagen type I alpha 1 chain; PDGFR, platelet-derived growth factor receptors; TIMP1, tissue inhibitor matrix metalloproteinase 1; GDF15, growth differentiation factor 15; GFRAL, glial cell-derived neurotrophic factor family receptor alpha-like; NCD, normal chow diet mice group; HFD, high-fat diet mice group; MMP-9, matrix metalloproteinase-9; GAPDH, 3-phosphate dehydrogenase; SEM, standard error of the mean; AKT, protein kinase B.

of Tgfβ, αSma, Col1a1, Pdgfr, Timp1, Gdf15, and Gfral in the lung tissues of the HFD fed mice compared to those of the NCD fed mice (*Figure 4A*,*4B*). Western blot was used to detect the levels of proteins related to DAVID clustering terms, and the results showed increased protein levels of p-AKT/AKT, β-catenin, and GDF15 in the lung tissues of the HFD fed mice compared to those of the NCD fed mice (*Figure 4C*). Also, western blot was used to detect the levels of proteins related to lung fibrosis, and the results showed increased protein levels of MMP-9 and αSMA in the lung tissues of the HFD fed mice compared to those of the NCD fed mice (*Figure 4D*).

Discussion

The results of animal experiments conducted in this study demonstrated that HFD-induced obesity may accelerate the risk of lung fibrosis and lung cancer. Moreover, we found significantly distinct alteration of the genes and proteins related to lung fibrosis and lung cancer expressed in the lung tissues of HFD-induced obese mice compared to those in control tissues.

The volcano plot revealed several distinct genes such as *Ttpa* involved in increased inflammatory response (20). Additionally, we identified the top 15 genes which were increased including *Zbtb16*; the transcription factor PLZF (*Zbtb16*) directs the effector process of NKT cells, a well characterized preserved population of T cells (21). Moreover, FK506-binding protein 5 (*FKBP5*) plays a role in immunoregulation, apoptotic response, and also is highly expressed in T lymphocytes (22). Increased level of *Hif3a* leads to abnormal alveoli structure related to pulmonary function (23). Increased level of *Angptl4* boosts pulmonary tissue leakiness and aggravates inflammation-induced lung tissue damage (24). Increased expression of *Lox* is involved in impaired pulmonary alveolarization (25). Elevated expression of *Pde2a* cause the high level of iNOS and alveolar inflammation in lung (26). Also, increased expression of *Pdk4* in lung pericytes promotes lung tumorigenesis by regulating pyruvate dehydrogenase (27). Considering this evidence, the lung tissues of the HFD fed mice tend to show increased expression of cancer- and lymphocyte-related genes. Moreover, we selected the top 15 decreased genes, including *Rbp*7, a member of the cellular retinol-binding protein family, is known to play a regulatory role in the cellular antioxidant process together with the cofactor PPAR gamma (28). The reduced expression of *Lzts1* is involved in tumorigenesis of lung cancer (29). Decreased expression of *Wnt7a* increases small lung cancer cell proliferation (30). The reduced expression of *Glp1r* leads to increased pulmonary inflammation (31). Also, *Cyp26b1* is known to be highly expressed in lung endothelial cells, and its loss results in a reduction in alveolar type 1 cells, leading to impaired alveolar inflation (32). As mentioned above, the lung of the HFD fed mice is associated with increased immune and inflammatory responses and cancer-related signaling. Given this evidence, the lung tissues of the HFD fed mice tend to show decreased expression of antioxidant response-related, cancer protective, pulmonary alveolarization and pulmonary alveolar cell protective genes.

Additionally, we found significantly highly enriched GO terms and KEGG pathways in the lungs of HFD fed mice. The top GO term was positive regulation of the nitrogen compound metabolic process. Nitrogen is the most common gas in the lung, where the nitrogen oxidation-reduction processes occur continuously. Unlike other gases in the lung, nitrogen reacts least with hemoglobin, and nitrogen oxide produced by nitric oxide synthase (NOS) activity is considered as a NO free radical (33). The nitrogen process is considered as critical in killing microbes (33). Nitrogen synthesizes various molecules, including amino acids and ammonia, and influences the growth of lymphocytes and cancer cells (33). A recent study reported that numerous types of cancer cells have increased demands on nitrogen sources, especially amino acids, and the lack of amino acids is considered a metabolic checkpoint for immunity in cancer (34). Moreover, one study has suggested that the control of nitrogen metabolism contributes to cellular metabolism in immune, stromal, and cancer cells (35). Considering the result from the previous studies, the lungs of the HFD fed mice are closely related to changes in nitrogen metabolism compared to the lungs of the NCD fed mice. The relationship between nitrogen metabolism regulation and HFD implies that a HFD may affect lung cancer progression through alterations in nitrogen-related processes.

We also identified G-protein coupled receptor (GPCR) signaling as an enriched GO term. GPCRs in airway smooth muscle are direct therapeutic targets of anti-asthmatic drugs in disorders such as asthma to attenuate airway inflammation and promote airway remodeling (36). Furthermore, KEGG analysis identified the following significant terms: small cell lung cancer, FC gamma R mediated phagocytosis, T-cell receptor signaling pathway,

WNT signaling pathway, VEGF signaling pathway, NOTCH signaling pathway, apoptosis, non-small cell lung cancer, and NK-cell mediated cytotoxicity. VEGF/HIF-1α signaling is involved in cancer metastasis, cancer growth, and progression of tumor vessels (37). Rap1 signaling regulates the metastasis of non-small cell lung cancer and cell proliferation of lung adenocarcinoma (38). $CD8^+$ T cell infiltration is an important issue in lung adenocarcinoma and small cell lung cancer (39). Moreover, NK cell cytotoxicity and NK cell contractility aggravate the progression of lung adenocarcinoma (40). Our DAVID data revealed significant clusters, including VEGF signaling, HIF-1 signaling, and Rap 1 signaling. Based on it, the lungs of HFD mice are involved in significant signaling related to cancer metastasis, invasion, lymphocyte activation, cancer growth, leukocyte stimulation, tumor vessel formation, cell proliferation, and apoptosis.

Furthermore, in the lung tissues of HFD fed mice, we found strong genetic connections among *Hspa5*, *Hsp90aa1*, *Dkc1*, *Dnajc21*, *Myc*, *Rela*, *Cdk4*, and *Pdk4* using the STRING tool. *Dkc1* is involved in lung adenocarcinoma, cell senescence, metastasis, apoptosis and angiogenesis in cancer (41). Moreover, *Cdk4* can be used as a biomarker for detecting lung and head cancers (42), while *Cdk4* inhibitors can be used to treat non-small cell lung cancer. As mentioned above, considering that lung cancer-related genes are central hubs that connect with other proteins, the lungs of HFD mice may show increased expression of the abovementioned lung cancer genes, which will increase the risk of lung cancer in the future.

Additionally, our PCR data revealed increased lung fibrosis-related genes, including Tgfβ and Gdf15, in the lungs of the HFD fed mice. Pulmonary fibrosis, such as idiopathic pulmonary fibrosis, is associated with an increased risk of lung cancer and has been shown to be involved in lung cancer through common pathogenic biological mechanisms (43). The increased expression of Tgfβ leads to lung fibrosis and airway remodeling, including abnormal extracellular matrix deposition via promoting fibroblast activation (44). The increased expression of Gdf15 and Gfral, as receptors for Gdf15, accelerates the activation of macrophages and fibroblasts and leads to lung fibrosis (45). Moreover, αSma upregulates fibroblast contractile activity and Tgfβ activation, leading to lung fibrosis (46). Pdgfr and Timp1 regulate lung fibrosis and vascular remodeling in lung fibrosis (47). As a result, our PCR data showed the genes expressed in the lungs of HFD mice tends to induce lung fibrosis.

However, our results had a limitation. We did not perform specific histopathological analysis of the lung tissues, because we focused on the screening of genes related to lung fibrosis and lung cancer and confirmed the relationship between lung function and obesity induced by HFD. Therefore, we need to conduct specific histological analysis of the lung tissues to identify if the HFD affect lung structure describing lung function.

Despite the limitation, our results showed the genetic alteration and the changes of significant molecular signaling of the lung tissue in the HFD fed mice. It suggested that HFD-induced obesity contributes to an increased risk of lung fibrosis and lung cancer. Further studies are needed to elucidate the effect of HFD-induced obesity on the risk of lung fibrosis and lung cancer in humans including healthy people and patients with lung disease.

Conclusions

This study analyzed genetic alteration and molecular signaling changes of the lung tissue in the HFD induced obese mouse model through the transcriptomic and molecular analysis. Thus, our results showed that HFD contributes to an increased risk of lung fibrosis and lung cancer. Therefore, we propose that the genetic modulation and the molecular regulation of target pathways are essential to suppress pulmonary fibrosis in obese patients.

Acknowledgments

The authors acknowledge Biorender.com for creating the figures.

Funding: This study was supported by grants from the National Research Foundation of Korea (NRF) (No. RS-2022-NR069292 to J.S. and No. RS-2022-NR069592 to O.Y.K.).

Footnote

Reporting Checklist: The authors have completed the ARRIVE reporting checklist. Available at https://tlcr.amegroups.com/article/view/10.21037/tlcr-24-659/rc

Data Sharing Statement: Available at https://tlcr.amegroups.com/article/view/10.21037/tlcr-24-659/dss

Peer Review File: Available at https://tlcr.amegroups.com/article/view/10.21037/tlcr-24-659/prf

Conflicts of Interest: All authors have completed the ICMJE uniform disclosure form (available at https://tlcr.amegroups.com/article/view/10.21037/tlcr-24-659/coif). The authors have no conflicts of interest to declare.

Ethical Statement: The authors are accountable for all aspects of the work in ensuring that questions related to the accuracy or integrity of any part of the work are appropriately investigated and resolved. Experiments were performed under a project license (CNU IACUC-H-2022-8) granted by Animal Ethics Committee of Chonnam National University (CNU), in compliance with the 96 Guidance for Animal Experiments for the care and use of animals.

References

1. Wang L, Wang H, Zhang B, et al. Elevated Fat Intake Increases Body Weight and the Risk of Overweight and Obesity among Chinese Adults: 1991-2015 Trends. Nutrients 2020;12:3272.
2. Zhang X, Liu Y, Shao H, et al. Obesity Paradox in Lung Cancer Prognosis: Evolving Biological Insights and Clinical Implications. J Thorac Oncol 2017;12:1478-88.
3. Barbi J, Patnaik SK, Pabla S, et al. Visceral Obesity Promotes Lung Cancer Progression-Toward Resolution of the Obesity Paradox in Lung Cancer. J Thorac Oncol 2021;16:1333-48.
4. Hidayat K, Du X, Chen G, et al. Abdominal Obesity and Lung Cancer Risk: Systematic Review and Meta-Analysis of Prospective Studies. Nutrients 2016;8:810.
5. Koh WP, Yuan JM, Wang R, et al. Body mass index and smoking-related lung cancer risk in the Singapore Chinese Health Study. Br J Cancer 2010;102:610-4.
6. Leone N, Courbon D, Thomas F, et al. Lung function impairment and metabolic syndrome: the critical role of abdominal obesity. Am J Respir Crit Care Med 2009;179:509-16.
7. Lee AS, Mira-Avendano I, Ryu JH, et al. The burden of idiopathic pulmonary fibrosis: an unmet public health need. Respir Med 2014;108:955-67.
8. Miyake Y, Sasaki S, Yokoyama T, et al. Dietary fat and meat intake and idiopathic pulmonary fibrosis: a case-control study in Japan. Int J Tuberc Lung Dis 2006;10:333-9.
9. Sin DD, Jones RL, Man SF. Obesity is a risk factor for dyspnea but not for airflow obstruction. Arch Intern Med 2002;162:1477-81.
10. Watson RA, Pride NB. Postural changes in lung volumes and respiratory resistance in subjects with obesity. J Appl Physiol (1985) 2005;98:512-7.
11. Bolger AM, Lohse M, Usadel B. Trimmomatic: a flexible trimmer for Illumina sequence data. Bioinformatics 2014;30:2114-20.
12. Maia LA, Cruz FF, de Oliveira MV, et al. Effects of Obesity on Pulmonary Inflammation and Remodeling in Experimental Moderate Acute Lung Injury. Front Immunol 2019;10:1215.
13. Togashi Y, Shirakawa J, Okuyama T, et al. Evaluation of the appropriateness of using glucometers for measuring the blood glucose levels in mice. Sci Rep 2016;6:25465.
14. Dobin A, Davis CA, Schlesinger F, et al. STAR: ultrafast universal RNA-seq aligner. Bioinformatics 2013;29:15-21.
15. Trapnell C, Roberts A, Goff L, et al. Differential gene and transcript expression analysis of RNA-seq experiments with TopHat and Cufflinks. Nat Protoc 2012;7:562-78.
16. Liberzon A, Subramanian A, Pinchback R, et al. Molecular signatures database (MSigDB) 3.0. Bioinformatics 2011;27:1739-40.
17. Shannon P, Markiel A, Ozier O, et al. Cytoscape: a software environment for integrated models of biomolecular interaction networks. Genome Res 2003;13:2498-504.
18. Warde-Farley D, Donaldson SL, Comes O, et al. The GeneMANIA prediction server: biological network integration for gene prioritization and predicting gene function. Nucleic Acids Res 2010;38:W214-20.
19. Huang da W, Sherman BT, Lempicki RA. Systematic and integrative analysis of large gene lists using DAVID bioinformatics resources. Nat Protoc 2009;4:44-57.
20. Schock BC, Van der Vliet A, Corbacho AM, et al. Enhanced inflammatory responses in alpha-tocopherol transfer protein null mice. Arch Biochem Biophys 2004;423:162-9.
21. Savage AK, Constantinides MG, Han J, et al. The transcription factor PLZF directs the effector program of

the NKT cell lineage. Immunity 2008;29:391-403.
22. Zhao J, Long X, Yang Y, et al. Identification and characterization of a pig FKBP5 gene with a novel expression pattern in lymphocytes and granulocytes. Anim Biotechnol 2019;30:302-10.
23. Kawahata T, Tanaka K, Oyama K, et al. HIF3A gene disruption causes abnormal alveoli structure and early neonatal death. PLoS One 2024;19:e0300751.
24. Li L, Chong HC, Ng SY, et al. Angiopoietin-like 4 Increases Pulmonary Tissue Leakiness and Damage during Influenza Pneumonia. Cell Rep 2015;10:654-63.
25. Kumarasamy A, Schmitt I, Nave AH, et al. Lysyl oxidase activity is dysregulated during impaired alveolarization of mouse and human lungs. Am J Respir Crit Care Med 2009;180:1239-52.
26. Rentsendorj O, Damarla M, Aggarwal NR, et al. Knockdown of lung phosphodiesterase 2A attenuates alveolar inflammation and protein leak in a two-hit mouse model of acute lung injury. Am J Physiol Lung Cell Mol Physiol 2011;301:L161-70.
27. Yu S, Li Y, Ren H, et al. PDK4 promotes tumorigenesis and cisplatin resistance in lung adenocarcinoma via transcriptional regulation of EPAS1. Cancer Chemother Pharmacol 2021;87:207-15.
28. Woll AW, Quelle FW, Sigmund CD. PPARγ and retinol binding protein 7 form a regulatory hub promoting antioxidant properties of the endothelium. Physiol Genomics 2017;49:653-8.
29. Toyooka S, Fukuyama Y, Wistuba II, et al. Differential expression of FEZ1/LZTS1 gene in lung cancers and their cell cultures. Clin Cancer Res 2002;8:2292-7.
30. Xu X, Xu S, Wei Z, et al. Wnt7a inhibits transformed cell proliferation while promoting migration and invasion in non-small cell lung cancer. Transl Cancer Res 2020;9:4666-75.
31. Sato T, Shimizu T, Fujita H, et al. GLP-1 Receptor Signaling Differentially Modifies the Outcomes of Sterile vs Viral Pulmonary Inflammation in Male Mice. Endocrinology 2020;161:bqaa201.
32. Daniel E, Barlow HR, Sutton GI, et al. Cyp26b1 is an essential regulator of distal airway epithelial differentiation during lung development. Development 2020;147:dev181560.
33. Hosios AM, Hecht VC, Danai LV, et al. Amino Acids Rather than Glucose Account for the Majority of Cell Mass in Proliferating Mammalian Cells. Dev Cell 2016;36:540-9.
34. Lukey MJ, Katt WP, Cerione RA. Targeting amino acid metabolism for cancer therapy. Drug Discov Today 2017;22:796-804.
35. Olenchock BA, Rathmell JC, Vander Heiden MG. Biochemical Underpinnings of Immune Cell Metabolic Phenotypes. Immunity 2017;46:703-13.
36. Kalavantavanich K, Schramm CM. Dexamethasone potentiates high-affinity beta-agonist binding and g(s)alpha protein expression in airway smooth muscle. Am J Physiol Lung Cell Mol Physiol 2000;278:L1101-6.
37. Chen Z, Zhao L, Zhao F, et al. Tetrandrine suppresses lung cancer growth and induces apoptosis, potentially via the VEGF/HIF-1α/ICAM-1 signaling pathway. Oncol Lett 2018;15:7433-7.
38. Kan J, Fu B, Zhou R, et al. He-Chan Pian inhibits the metastasis of non-small cell lung cancer via the miR-205-5p-mediated regulation of the GREM1/Rap1 signaling pathway. Phytomedicine 2022;94:153821.
39. Imamura K, Tomita Y, Sato R, et al. Clinical Implications and Molecular Characterization of Drebrin-Positive, Tumor-Infiltrating Exhausted T Cells in Lung Cancer. Int J Mol Sci 2022;23:13723.
40. Zheng QW, Ni QZ, Zhu B, et al. PPDPF promotes lung adenocarcinoma progression via inhibiting apoptosis and NK cell-mediated cytotoxicity through STAT3. Oncogene 2022;41:4244-56.
41. Kan G, Wang Z, Sheng C, et al. Inhibition of DKC1 induces telomere-related senescence and apoptosis in lung adenocarcinoma. J Transl Med 2021;19:161.
42. Banerjee J, Pradhan R, Gupta A, et al. CDK4 in lung, and head and neck cancers in old age: evaluation as a biomarker. Clin Transl Oncol 2017;19:571-8.
43. Perrotta F, Chino V, Allocca V, et al. Idiopathic pulmonary fibrosis and lung cancer: targeting the complexity of the pharmacological interconnection. Expert Rev Respir Med 2022;16:1043-55.
44. Tatler AL, Jenkins G. TGF-β activation and lung fibrosis. Proc Am Thorac Soc 2012;9:130-6.
45. Takenouchi Y, Kitakaze K, Tsuboi K, et al. Growth differentiation factor 15 facilitates lung fibrosis by activating macrophages and fibroblasts. Exp Cell Res 2020;391:112010.
46. Sun KH, Chang Y, Reed NI, et al. α-Smooth muscle actin is an inconsistent marker of fibroblasts responsible for force-dependent TGFβ activation or collagen production across multiple models of organ fibrosis. Am J Physiol Lung Cell Mol Physiol 2016;310:L824-36.

47. Biasin V, Crnkovic S, Sahu-Osen A, et al. PDGFRα and αSMA mark two distinct mesenchymal cell populations involved in parenchymal and vascular remodeling in pulmonary fibrosis. Am J Physiol Lung Cell Mol Physiol 2020;318:L684-97.

Cite this article as: Park J, Jo D, Choi SY, Oh S, Jung YS, Kim OY, Song J. Long-term high fat diet aggravates the risk of lung fibrosis and lung cancer: transcriptomic analysis in the lung tissues of obese mice. Transl Lung Cancer Res 2024;13(12):3513-3525. doi: 10.21037/tlcr-24-659

